

# Design and Implementation of a Bidirectional DC-DC Forward/Flyback Converter with Leakage Energy Recycled

Yi-Ju Lu, Tsorng-Juu Liang, *Fellow, IEEE*, Ci-Hong Lin and Kai-Hui Chen

Green Energy Electronics Research Center (GREERC)/ Advanced Optoelectronic Technology Center (AOTC)

Department of Electrical Engineering, National Cheng Kung University, Tainan, Taiwan

Email: tjliang@mail.ncku.edu.tw

**Abstract**—A bidirectional interleaved forward-flyback DC-DC converter with leakage energy recycled is proposed in this paper. The proposed converter uses two transformers to reduce the current stress on the power components to reduce the conduction loss and improve the efficiency. When the proposed converter is operated in the step-up mode, the voltage across switches is clamped at the input voltage, and the leakage energy is recycled to the voltage source. When the proposed converter is operated in the step-down mode, the voltage of switches is clamped at the input voltage, and the leakage energy is recycled to the clamping capacitor or the voltage source. As the proposed converter is based on flyback converter, it is characterized with simple structure. Since the leakage inductance energy is recycled, the conversion efficiency is improved compared to conventional flyback converter. Finally, a laboratory prototype circuit with 200 V/24 V and output power 500 W is implemented to verify the feasibility of the proposed converter. The highest efficiency in the step-up and step-down stage is 92.3% and 95.5% respectively.

**Keywords**—forward/flyback converter, leakage energy recycled, bidirectional converter

## I. INTRODUCTION

The renewable energies, such as photovoltaic power, wind power, and ocean current, are not stable compared to the conventional power generation system. To overcome the unstable drawbacks of renewable energies, battery is treated as an importance energy storage component in the renewable power system. The bidirectional DC-DC converter is required to regulated the power between the battery and dc-bus in the battery integrated renewable energy system. When the green energy generates higher energy than the need for load, surplus energy is transferred from the DC bus to the battery through the bidirectional DC-DC converter. When the green energy can't provide sufficient energy to the load, the battery releases the stored energy to the DC bus. Therefore, the load can receive stable and sufficient energy and is not affected by the unstable green energy.

The bidirectional DC-DC converter can be divided into non-isolated topology and isolated topology. The non-isolated topology is low cost and easy to design [1]-[3]. However, for the sake of the safety consideration, an isolated topology is required. The forward-type isolated bidirectional converter has been proposed [4]-[6]. However, the forward type converter need additional inductor to store energy, the volume of circuit is increase. The bidirectional flyback DC-DC converter stores

energy in the transformer, the circuit volume can be reduced. But, this topology will impact by leakage inductance due to the air gap. In order to solve these problems. The interleaved bidirectional DC-DC forward/flyback converter with leakage energy recycled is proposed in this paper. The proposed converter use interleaved topology to reduce the current stress and recycle the leakage energy to increase efficiency.

## II. OPERATING PRINCIPLE ANALYSIS

Fig. 1 shows the proposed bidirectional forward-flyback converter with leakage energy recycled. The interleaved topology can reduce the current stress as well as the current ripple of the main switches and the transformers. Compared with the single transformer flyback converter, the proposed converter is suitable for higher power applications. Besides, the diodes are used to clamp the voltage and recycle the leakage energy. The operating principle of the proposed bidirectional forward-flyback converter in step-down and step-up modes are derived as follow.

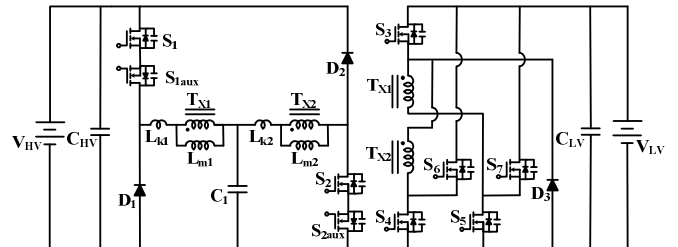


Fig. 1. The topology of the proposed converter

- *Step-up mode:*

Fig. 2 shows the equivalent circuit in step-up mode. When the proposed converter operated in step-up mode,  $S_3$ ,  $S_4$ , and  $S_5$  are the main switches. The diode  $D_1$  and  $D_2$  are used for rectifiers, the anti-parallel diode of  $S_6$  and  $S_7$  and the diode  $D_3$  are used to recycle leakage energy. In order to prevent current flow through the anti-parallel diode of  $S_1$  and  $S_2$ ,  $S_{1aux}$  and  $S_{2aux}$  are always turned off in this stage. By adjusting the duty ratio of  $S_3$ ,  $S_4$ , and  $S_5$ , the voltage gain can be changed and the energy can be transfer from  $V_{LV}$  to  $V_{HV}$ . Fig. 3 shows the key waveforms of step-up mode.



• *Step-down mode:*

In step-down stage, the main switches are  $S_1$  and  $S_2$ . The switches  $S_4, S_5, S_6,$  and  $S_7$  and the diode  $D_3$  are used for rectifier. The diodes  $D_1$  and  $D_2$  are used to recycle leakage energy. The switches  $S_{1aux}$  and  $S_{2aux}$  are always turned on, and the switch  $S_3$  is always turned off. The equivalent circuit in step-down stage is shown in Fig. 5 and the key waveforms of step-down stage are shown in Fig. 6. Since the operating modes from  $t_0$  to  $t_5$  is symmetrical with  $t_6$  to  $t_{10}$ .

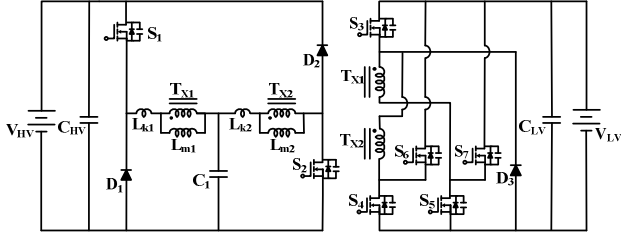


Fig. 5. The equivalent circuit of the proposed converter in step-down mode

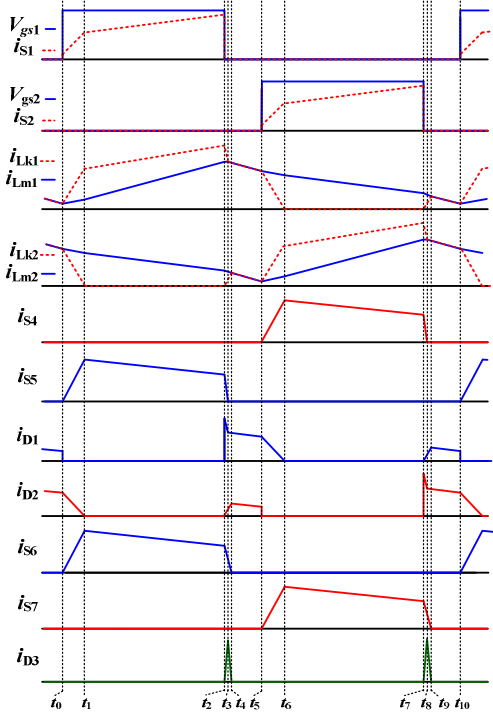


Fig. 6. Key waveforms in step-down stage

*Mode 1: [t<sub>0</sub>~t<sub>1</sub>]*

During this interval, the switch  $S_1, S_5,$  and  $S_6$  are turned on and the switch  $S_2, S_4,$  and  $S_7$  are turned off. The equivalent circuit of mode 1 is shown in Fig. 7 (a).  $V_{HV}$  provides energy to the capacitor  $C_1$  and provides energy to  $V_{LV}$  through the transformer  $T_{X1}$  and the switch  $S_5$  and  $S_6$ . The magnetizing inductance  $L_{m1}$  and the leakage inductance  $L_{k1}$  are charged by  $V_{HV}$ , so the current  $i_{Lm1}$  and  $i_{Lk1}$  increase linearly. The magnetizing inductance  $L_{m2}$  releases energy to  $V_{LV}$  through the transformer  $T_{X2}$  and the switch  $S_5$  and  $S_6$ . The leakage inductance  $L_{k2}$  releases energy to  $V_{HV}$  through the diode  $D_2$ . Therefore, the current  $i_{Lm2}$  and  $i_{Lk2}$

decrease linearly. This mode ends when the current  $i_{Lk2}$  decrease to zero.

*Mode 2: [t<sub>1</sub>~t<sub>2</sub>]*

During this interval, the switch  $S_1, S_5,$  and  $S_6$  are turned on, switch  $S_2, S_4,$  and  $S_7$  are turned off. The equivalent circuit of mode 2 is shown in Fig. 7 (b).  $V_{HV}$  provides energy to the capacitor  $C_1$  and provides energy to  $V_{LV}$  through the transformer  $T_{X1}$  and the switch  $S_5$  and  $S_6$ . The magnetizing inductance  $L_{m1}$  and leakage inductance  $L_{k1}$  are charged by  $V_{HV}$ , so the current  $i_{Lm1}$  and  $i_{Lk1}$  increase linearly. The magnetizing inductance  $L_{m2}$  releases energy to  $V_{LV}$  through the transformer  $T_{X2}$  and the switch  $S_5$  and  $S_6$ . This mode ends when switch  $S_1$  is turned off.

*Mode 3: [t<sub>2</sub>~t<sub>3</sub>]*

During this interval, the switch  $S_5$  and  $S_6$  are turned on, the switches  $S_1, S_2, S_4,$  and  $S_7$  are turned off. The magnetizing inductance  $L_{m2}$  releases energy to  $V_{LV}$  through the transformer  $T_{X2}$ . The equivalent circuit of mode 3 is shown in Fig. 7 (c). In the beginning, the values of  $i_{S5}$  and  $i_{S6}$  are the same. The difference between  $i_{S5}$  and  $i_{S6}$  goes through the diode  $D_3$  since the current  $i_{Lk1}$  decreases faster than  $i_{Lk2}$  and the low voltage side current  $i_{S5}$  decreases faster than  $i_{S6}$ . When the diode  $D_3$  conduction, the voltage of  $T_{X1}$  is clamped at zero, the magnetizing inductance current  $i_{Lm1}$  keeps a constant. The leakage inductance  $L_{k1}$  releases energy to capacitor  $C_1$  through the diode  $D_1$ . The current  $i_{Lk1}$  decrease linearly. The leakage inductance  $L_{k2}$  is charged by  $L_{m2}$ . The current  $i_{Lk2}$  increase linearly. This mode ends when the value of current  $i_{Lk1}$  is equal to current  $i_{Lm1}$ .

*Mode 4: [t<sub>3</sub>~t<sub>4</sub>]*

During this interval, the switch  $S_6$  is turned on and the switches  $S_1, S_2, S_4, S_5,$  and  $S_7$  are turned off. The equivalent circuit of mode 4 is shown in Fig. 7 (d). The magnetizing inductance  $L_{m1}$  and leakage inductance  $L_{k1}$  release energy to the capacitor  $C_1$  through the diode  $D_1$ , so the current  $i_{Lm1}$  and  $i_{Lk1}$  decrease linearly. Because the current  $i_{Lm1}$  is equal to current  $i_{Lk1}$ , the transformer  $T_{X1}$  is decoupled. The  $V_{LV}$  side voltage of transformer  $T_{X2}$  is equal to  $V_{LV}$ . The magnetizing inductance  $L_{m2}$  releases energy to  $V_{LV}$  through the transformer  $T_{X2}$ , the switch  $S_6$ , and the diode  $D_3$ , so the current  $i_{Lm2}$  decrease linearly. The leakage inductance  $L_{k1}$  is charged by  $L_{m2}$ , so the current  $i_{Lk2}$  increases linearly. This mode ends when the value of current  $i_{Lk2}$  equal to current  $i_{Lm2}$ .

*Mode 5: [t<sub>4</sub>~t<sub>5</sub>]*

During this interval, the switches  $S_1, S_2, S_4, S_5, S_6,$  and  $S_7$  are turned off. The equivalent circuit of mode 5 is shown in Fig. 7 (e). The magnetizing inductance  $L_{m1}$  and the leakage inductance  $L_{k1}$  release energy to the capacitor  $C_1$  through the diode  $D_1$ , so the currents  $i_{Lm1}$  and  $i_{Lk1}$  decrease linearly. The magnetizing inductance  $L_{m2}$  and the leakage inductance  $L_{k2}$  releases energy to  $V_{HV}$  through the diode  $D_2$ , so the current  $i_{Lm2}$  and  $i_{Lk2}$  decrease linearly. This mode ends when the switch  $S_2, S_4$  and  $S_7$  are turned on.

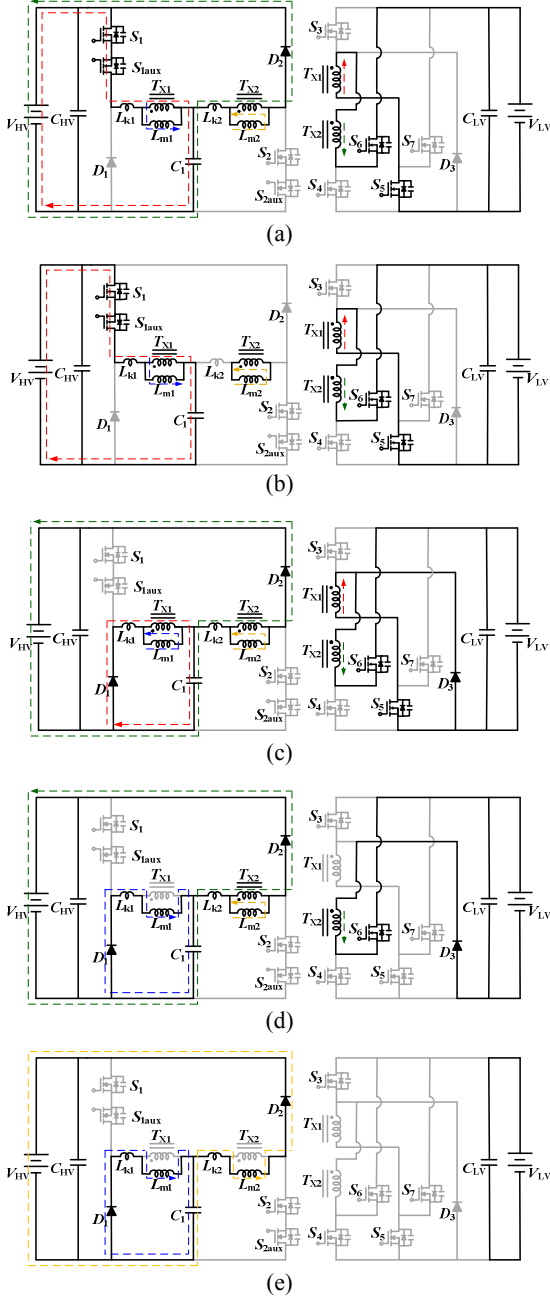


Fig. 7. Equivalent circuits of step-down mode operation (a) mode 1 (b) mode 2 (c) mode 3 (d) mode 4 (e) mode 5

### III. STEADY STATE ANALYSIS

To simplify the calculation, the leakage inductance and the transient time are ignored. Assume that the characteristic of transformers  $T_{X1}$  and  $T_{X2}$  are the same. In the step down mode, the voltage gain can be derived by the voltage-second balance of  $L_{m1}$ . It can be expressed as Eq. (1). Eq. (1) can be simplified as Eq. (2)

$$(V_{HV} - V_{C1})DT_s + (-V_{C1})\left(\frac{1-2D}{2}\right)T_s + \left[ (V_{C1})\frac{n_2}{n_1} - V_{LV} \right] \frac{n_1}{n_2} DT_s + (-V_{C1})\left(\frac{1-2D}{2}\right)T_s = 0 \quad (1)$$

$$\frac{V_{LV}}{V_{HV}} = \frac{4D-1}{2ND} \quad \text{where} \quad N = \frac{n_1}{n_2} \quad (2)$$

The magnetizing inductance  $L_{BCM}$  can be derived by calculating the magnetizing inductance current in BCM. The key waveforms of the magnetizing inductance current  $i_{Lm1}$  and the diode current  $i_{S7}$  are shown in Fig. 8. The average current of  $S_7$  is half of the output current. It can be derived as following:

$$i_{Lm1}(t_2) = i_{S7}(t_2) = \left[ NDV_{LV} + V_{HV}\left(\frac{1}{4} - D\right) \right] \frac{T_s N}{L_{m1}} \quad (3)$$

$$i_{Lm1}(t_3) = i_{S7}(t_3) = \frac{V_{HV}}{2L_{m1}} \left( \frac{1-2D}{2} \right) T_s N \quad (4)$$

$$i_{S7,ave} = \frac{I_{o,BCM}}{2} = \left[ \frac{V_{HV}(1-3D) + 2NDV_{LV}}{2} \right] N \frac{DT_s}{2L} \quad (5)$$

The boundary conduction inductance  $L_{m1,BCM}$  can be derived from Eq. (5) as shown in Eq. (6)

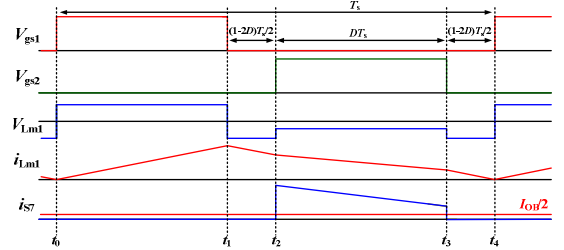


Fig. 8. Key waveforms of BCM in neglecting the effect of leakage inductance in step-down stage

$$L_{m1,BCM} = V_{HV} \left( \frac{V_{HV}}{2V_{HV} - NV_{LV}} \right)^2 \frac{NT_s}{8I_{o,BCM}} \quad (6)$$

When the proposed converter operates in step-up mode, the voltage gain can be derived as following:

$$V_{LV} \frac{n_1}{n_2} DT_s + \left(-\frac{1}{2}V_{HV}\right)(1-D)T_s = 0 \quad (7)$$

The Eq. (1) can be simplified as Eq. (2)

$$\frac{V_{HV}}{V_{LV}} = \frac{2ND}{1-D} \quad \left( N = \frac{n_1}{n_2} \right) \quad (8)$$

The key waveforms of the magnetizing inductance currents  $i_{Lm1}$ ,  $i_{Lm2}$ , and the diode currents  $i_{D1}$ ,  $i_{D2}$  are shown in Fig. 9. The average output diode currents  $i_{D1,ave}$  and  $i_{D2,ave}$  are equal to output current  $I_{o,BCM}$ . It can be expressed as Eq. (9).

$$i_{D1,pk} = i_{D2,pk} = i_{Lm1,pk} = i_{Lm2,pk} = \frac{2I_{o,BCM}}{1-D} \quad (9)$$

Because the converter operates in BCM, the total energy stored in magnetizing inductance will release to load.

$$\frac{P_{o,BCM}}{2} = \frac{V_o I_{o,BCM}}{2} = \frac{1}{2} L_{m1} i_{Lm1,pk}^2 f_s = \frac{1}{2} L_{m2} i_{Lm2,pk}^2 f_s \quad (10)$$

By substituting Eq. (9) to Eq. (10), the equation of boundary inductances  $L_{m1,BCM}$  and  $L_{m2,BCM}$  can be expressed as Eq. (11)

$$L_{m1,BCM} = L_{m2,BCM} = \frac{V_{HV}(1-D)^2}{4I_{o,BCM}f_s} \quad (11)$$

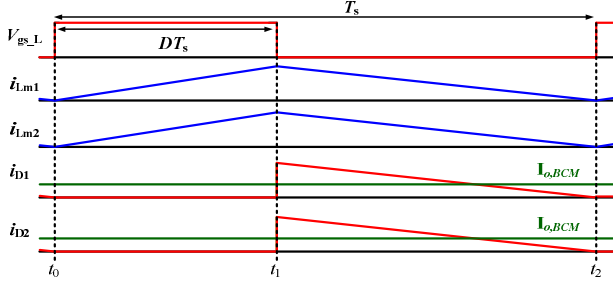


Fig. 9 Key waveforms of BCM in neglecting the effect of leakage inductance in step-up stage

The two values of  $L_{m,BCM}$  can be solved in step-down mode and step-up mode. The larger one is chosen. It can ensure that the converter meets the specifications. Because the smaller one leads the converter which operates in BCM at the power larger than specifications.

#### IV. EXPERIMENTAL RESULTS

A bidirectional DC-DC forward/flyback converter with leakage energy recycled is proposed and implementation in this paper. The specifications of the proposed converter are shown in Table 1. When the switch is turned off, the leakage energy can be recycled and the conversion efficiency is improved. The voltage across the switch can be clamped. As shown in Fig. 10 to Fig. 13, the voltage and current waveforms of key components are illustrated. The synchronous rectifier is added into the circuit to increase efficiency. Therefore, the highest efficiency in step-up and step-down stage is 92.7% and 95.5% respectively, as shown in Fig. 14 and Fig. 15.

Table 1. System Specifications

(a)	
Step-up Mode	
Input Voltage $V_{LV}$	24 V
Output Voltage $V_{HV}$	200 V
Rated Output Power	500 W
Switching Frequency	50 kHz

(b)	
Step-down Mode	
Input Voltage $V_{HV}$	200 V
Output Voltage $V_{LV}$	24 V
Rated Output Power	500 W
Switching Frequency	50 kHz

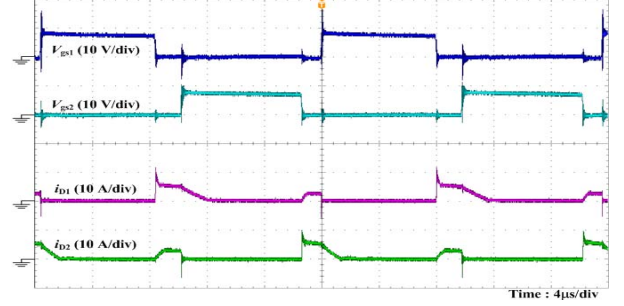


Fig. 10 The waveforms of  $V_{GS1}$ ,  $V_{GS2}$ ,  $i_{D1}$ , and  $i_{D2}$  (Step-down mode 500 W)

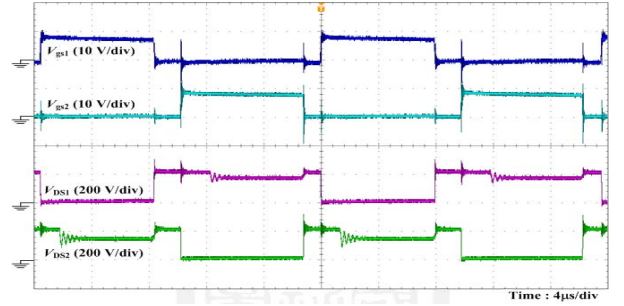


Fig. 11 The waveforms of  $V_{GS1}$ ,  $V_{GS2}$ ,  $V_{DS1}$ , and  $V_{DS2}$  (Step-down mode 500 W)

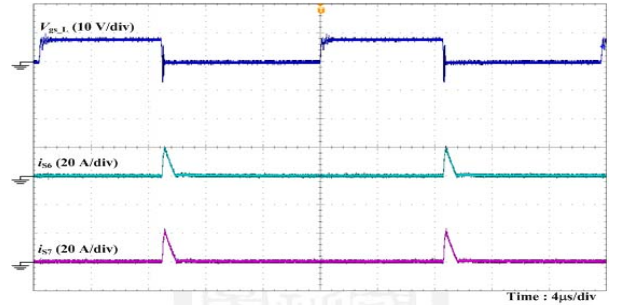


Fig. 12 The waveforms of  $V_{GS}$ ,  $i_{s6}$ , and  $i_{s7}$  (Step-up mode 500 W)

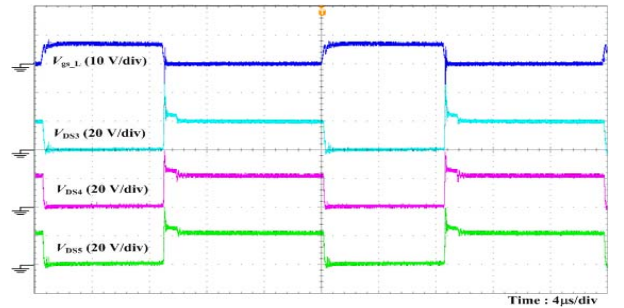


Fig.13 The waveforms of  $V_{GS1}$ ,  $V_{DS3}$ ,  $V_{DS4}$ , and  $V_{DS5}$  (Step-up mode 500 W)

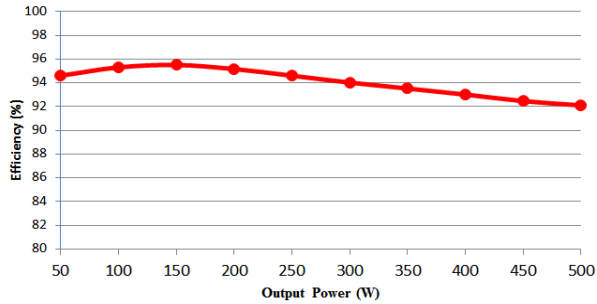


Fig. 14 The efficiency curve in step-down mode

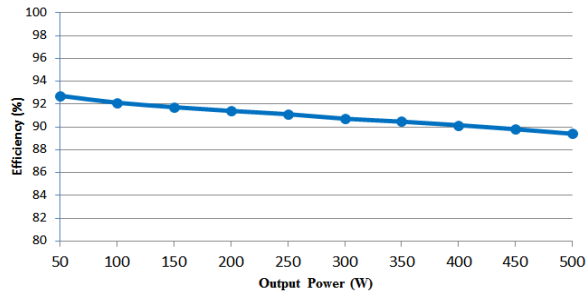


Fig.15 The efficiency curve in step-up mode

## V. CONCLUSIONS

The proposed bidirectional forward-flyback converter is composed of two transformers. The current stress and ripple can be reduced by using interleaved topology. The proposed converter uses the leakage energy recycled and the voltage clamping technologies to increase the efficiency. Besides, the current in low voltage is up to 20.83 A, the synchronous rectifier technology is added to reduce the conduction loss in heavy load. Finally, a laboratory prototype circuit with 200 V/24 V and output power 500 W is implemented to verify the feasibility of the proposed converter. The measured waveforms of prototype circuit correspond to the theory waveforms. When the converter is operated in step down stage, the highest efficiency is 95.5% and the full load efficiency is 92.1%. When the converter is operated in step-up stage, the highest efficiency is 92.3% and the full load efficiency is 90.3%.

## ACKNOWLEDGEMENT

The author gratefully acknowledge financial support from the Ministry of Science and Technology, Taiwan under project No. 105-2218-E-006 -009 - and No. 105-2221-E-006 -177 -MY2.

## REFERENCE

- [1] H. Ardi, R. R. Ahrabi, S. N. Ravadanegh, "Non-isolated bidirectional DC-DC converter analysis and implementation," *IET Power Electron.*, vol. 7, pp. 3033-3044, Dec. 2014.
- [2] H. L. Do, "Nonisolated Bidirectional Zero-Voltage-Switching DC-DC Converter," *IEEE Trans. on Power Electron.*, vol. 26, no. 9, pp. 2563-2569, Sep. 2011.
- [3] C. M. Hong, L. S. Yang, T. J. Liang, J. F. Chen, "Novel bidirectional DC-DC converter with high step-up/down voltage gain," in *IEEE Energy Conversion Congress and Exposition (ECCE)*, pp. 60-66, Sep. 2009.

- [4] H. Tao, J. L. Duarte, and M. A. M. Hendrix, "Three-Port Triple-Half-Bridge Bidirectional Converter With Zero-Voltage Switching," *IEEE Trans. on Power Electron.*, vol. 23, no. 2, pp. 782-792, Mar. 2008.
- [5] F. Z. Peng, Hui Li, G. J. Su, and J. S. Lawler, "A New ZVS Bidirectional DC-DC Converter for Fuel Cell and Battery Application," *IEEE Trans. on Power Electron.*, vol. 19, no. 6, pp. 54-65, Jan. 2004.
- [6] R. Ramachandran and M. Nymand, "A 98.8% efficient bidirectional full-bridge isolated dc-dc GaN converter," in *2016 IEEE Applied Power Electronics Conference and Exposition (APEC)*, pp. 609-614, Mar. 2016.
- [7] Y. T. Chen and S. Y. Wei, "A multiple-winding bidirectional flyback converter used in the solar system," in *Next-Generation Electronics (ISNE), 2013 IEEE International Symposium on*, pp. 130-133, Feb. 2013.
- [8] M. H. Todorovic, L. Palma, and P. Enjeti, "Design of a wide input range DC-DC converter with a robust power control scheme suitable for fuel cell power conversion," *IEEE Trans. on Industrial Electron.*, vol. 55, no. 3, pp. 1247-1255, Mar. 2008.
- [9] M. Delshad and H. Farzanehfard, "A new isolated bidirectional buck-boost PWM converter," *Power Electronic & Drive Systems & Technologies Conference (PEDSTC)*, 2010, pp. 41-45, Feb. 2010.
- [10] K. H. Chao and C. H. Huang, "Bidirectional DC-DC soft-switching converter for stand-alone photovoltaic power generation systems," *IET Power Electron.*, vol. 7, pp. 1557-1565, Jun. 2014.